Journal of Materials Chemistry A

Supporting Information

Design principles for platinum nanoparticles catalysing the electrochemical hydrogen evolution and oxidation reactions: edges are much more active than facets

C M Zalitis[a,b], A. R. Kucernak[a,†], Jonathan Sharman[b], and Ed Wright[b]

a. Imperial College London, Department of Chemistry, London, SW7 2AZ, United Kingdom.

b. Johnson Matthey Technology Centre, Blounts Court Road, Sonning Common, Reading, RG4 9NH, United Kingdom.

† Corresponding author, Ph:+44 20 75945831, e-mail: anthony@imperial.ac.uk.

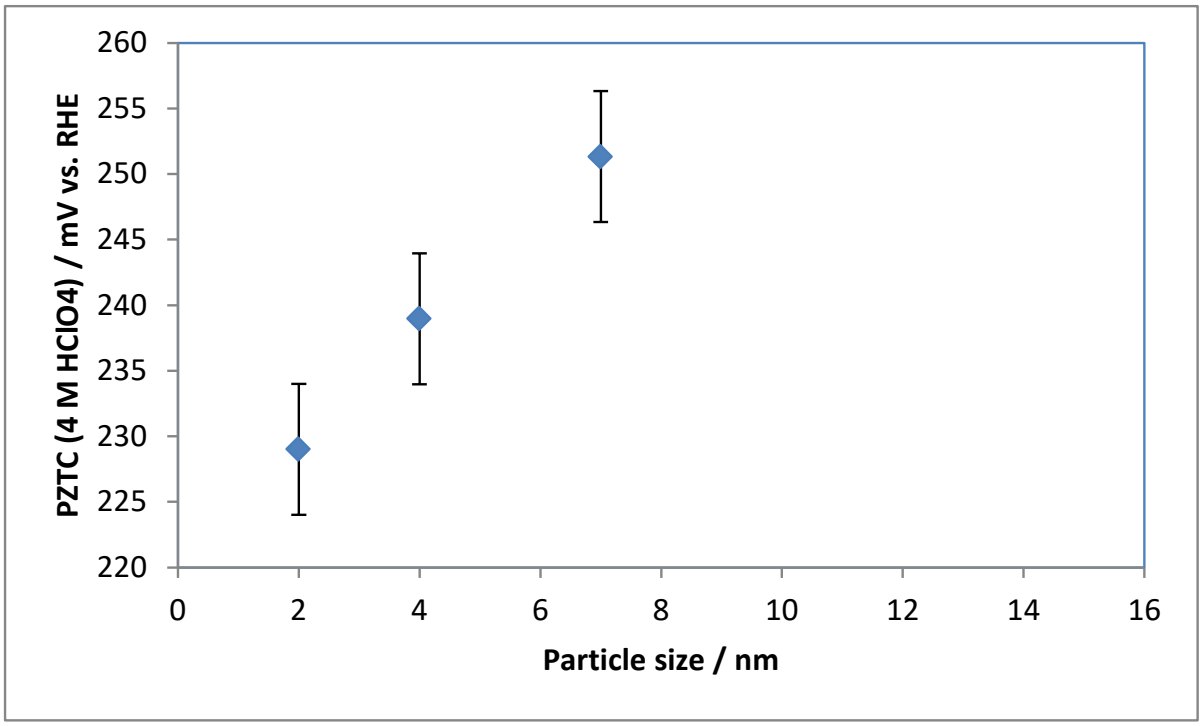

Figure 1. **PZTC as a function of particle diameter** Measurements performed for the three smallest particle size measured via the CO displacement method as described in [1]. As seen in Figure S3, there is a positive shift in PZTC with particle size.. Measurements performed using the CO technique in 4 mol dm^{-3} $HClO_4$ at 298 K. CE = Pt wire, RE = RHE.

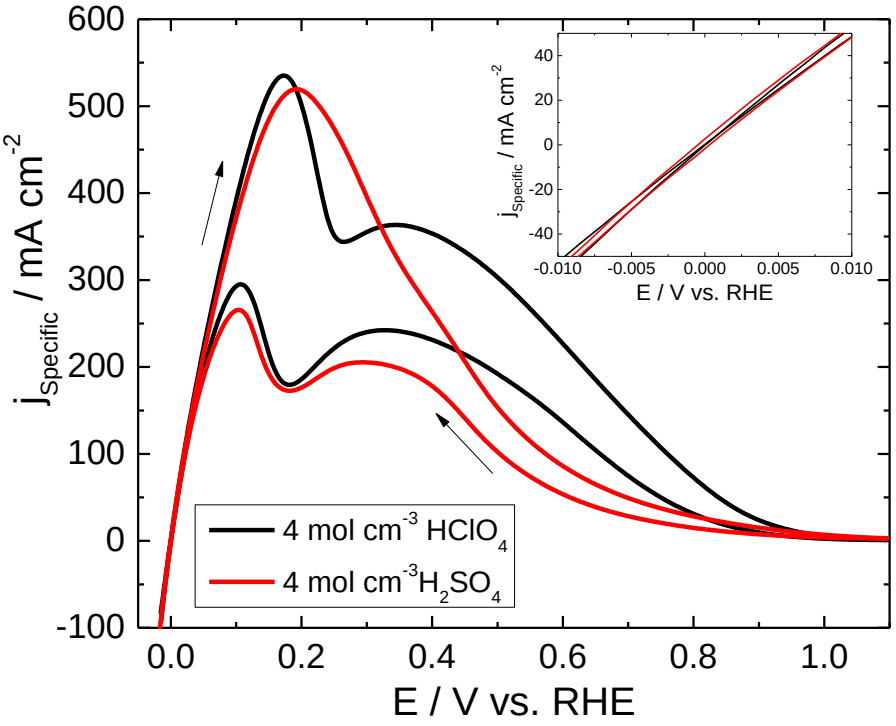

Figure 2. Voltammograms of the HOR/HER for 1.7μg_{Pt} cm^{-2} HiSpec 9100 60wt% Pt/C catalyst. Inset: Expansion of the micropolarisation region. The CVs were run in 4 mol dm^{-3} $HClO_4$ and H_2SO_4 at 10 mV s^{-1} at 298 K, 101 kPa H_2.

A

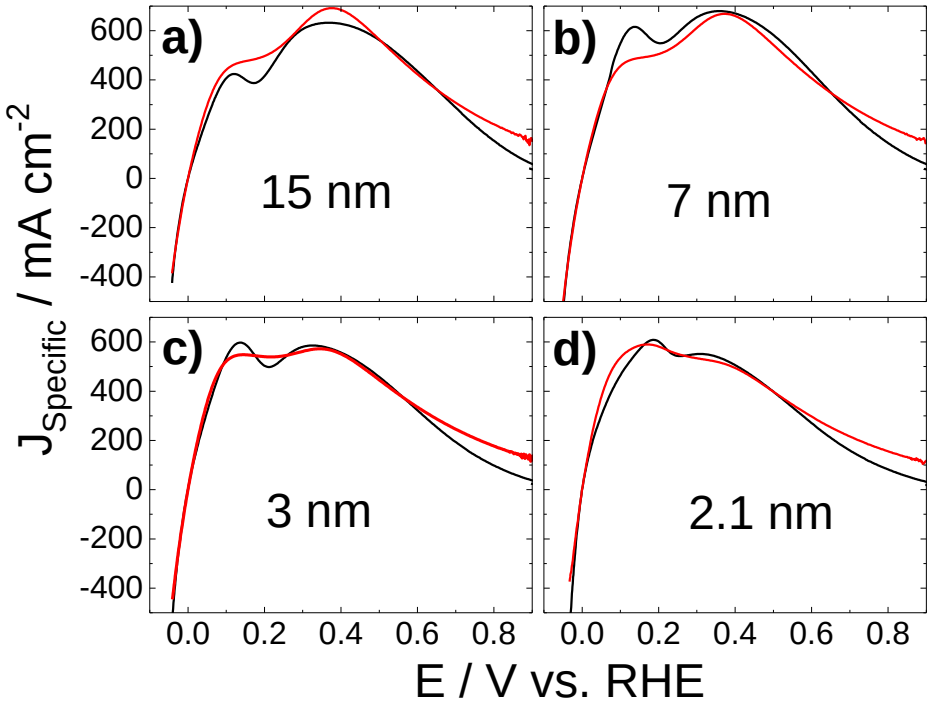

B

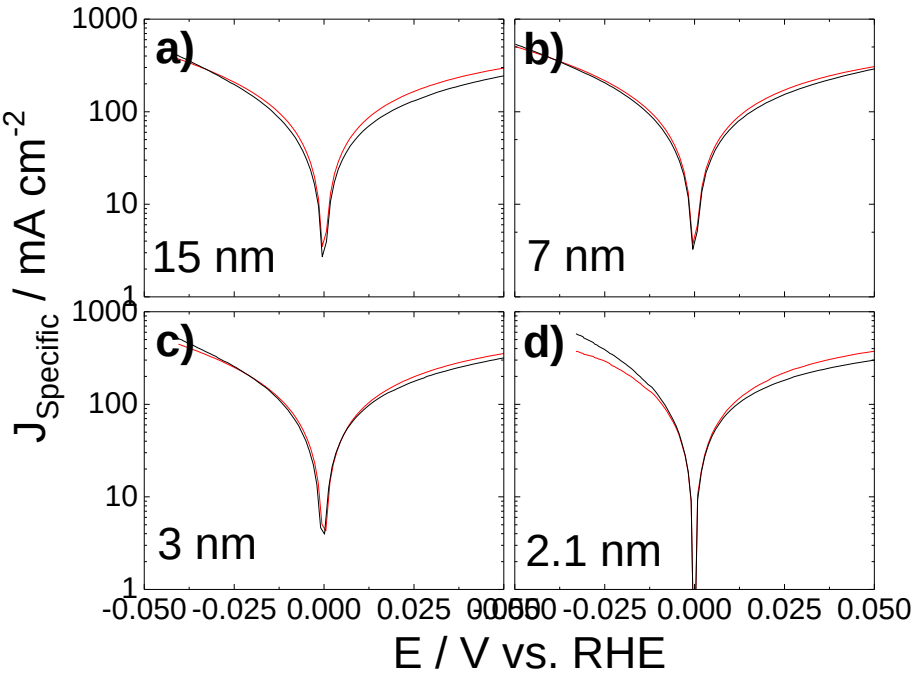

Figure 3. **Fit of response for forward voltametric scan. A.** Fit of the HOR/HER curves (red line) for the forward scan in Figure 3 from -0.02 – 0.5 V vs. RHE using a two site model (data: black line). B. Expansion of the fit close to the equilibrium potential. The data used was for the scan in the anodic direction (see text). Summary of the fitting results are provided in supplementary Table 3.

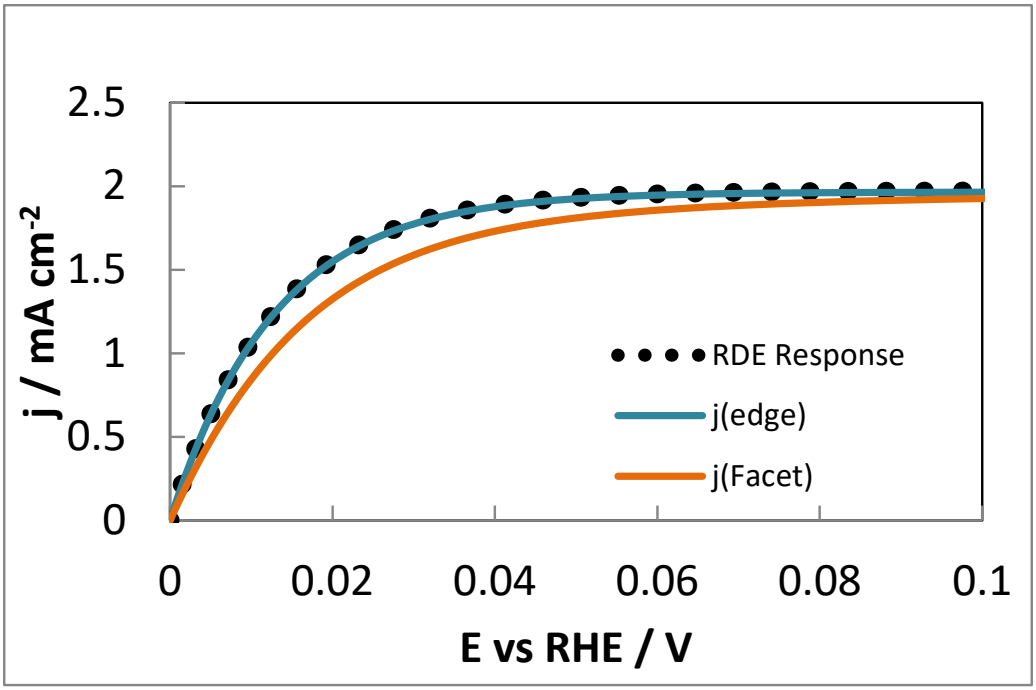

Figure 4. Calculated response for an RDE during the oxidation of hydrogen for an infinitely fast catalytic at 1600 RPM (dotted line). Calculated response for edge (blue) and facet (orange) under the same conditions utilising parameters from Table 2. Saturated 0.1 mol dm^{-3} $HClO_4$, 298K.

Table 1. **Oxide peak formation.** Peak position and peak area of oxide adsorption from the range of particles shown Figure 2

Size / nm	$O_{des,1}$ E /V vs. RHE	$O_{des,1}$ Q /mC cm^{-2}_{Spec}	$O_{des,1}$ Fraction	$O_{des,2}$ E /V vs. RHE	$O_{des,2}$ Q / mC cm^{-2}_{Spec}	$O_{des,2}$ Fraction
2.1	0.60	0.103	0.45	0.75	0.125	0.55
2.7	0.62	0.093	0.41	0.78	0.133	0.59
6.9	0.61	0.088	0.40	0.78	0.132	0.60
14.6	0.62	0.082	0.38	0.80	0.137	0.62

Table 2. **Parameters for peaks in HOR voltammetry.** Comparisons of peak current densities for the Pt/C catalysts of different particle sizes at 298 K in 4 mol dm^{-3} $HClO_4$.

Particle size /nm	$j_{Peak,low}$ /mA cm^{-2}_{Spec}	$j_{Peak,high}$ /mA cm^{-2}_{Spec}	$j_{Peak,high}$ / $j_{Peak,low}$
15	424	632	1.49
7	616	680	1.10
3	597	586	0.98
2.1	608	551	0.91

Calculating facet ratios for nanoparticles

Using the cubo-octahedron shape, the particle size can be related to the total number of atoms in the particle, Equation S.1 [2].

$$d = 1.11 d_{at} {N_t}^{1/3} \qquad \text{S.1}$$

And each facet can be related to the number of atoms along an edge (v) through equations S.2 - S.4.

$$N_H = 8((v-1)^3 - (v-2)^3) \qquad v \geq 2 \qquad \text{S.2}$$

$$N_S = 6\left(v^2 - 4(v-1)\right) \qquad v \geq 2 \qquad \text{S.3}$$

$$N_E = 24(v-1) + 12(v-2) \qquad v \geq 2 \qquad \text{S.4}$$

Where N_H, N_S and N_E are the number of atoms in the hexagonal Pt(111) facet, square Pt(100) facet and edge and corner sites, respectively. The number of atoms along an edge relates to the total number atoms through Equation S.5.

$$N_t = 16v^3 - 33v^2 + 24v - 6 \qquad \text{S.5}$$

For platinum, the radius of a metal atom is 0.1385 nm, so solving for v we find that a 1 nm particle requires v=3.258.

Figure 1 a) (main paper) shows the ratios of the different sites across a 1 – 16 nm particle size diameter range. Also shown is the sum of the facets: Pt(111) and Pt(100). As can be seen, the ratio of each surface site changes substantially across this range, with edge sites making up about 49% in 1.8 nm particles, and only 0.06% in 15 nm particles.

In order to calculate the ratio of peak currents, we assume the reaction is first order with respect to the available surface area and thus we equate the ratio of currents to the ratio of areas.

$$\frac{j_{peak,high}}{j_{peak,low}} = \frac{A_{Pt100}}{A_{Pt111}} = \frac{N_H}{N_S} = \frac{3(-2+v)^2}{4(7+3(-3+v)v)} \qquad v \geq 2 \qquad \text{S.6}$$

$$\frac{j_{peak,high}}{j_{peak,low}} = \frac{A_{Facet}}{A_{Edge}} = \frac{N_H+N_S}{N_E} = \frac{5v}{6} + \frac{2}{9}\left(-7 + \frac{2}{-4+3v}\right) \qquad v \geq 2 \qquad \text{S.7}$$

Hence we can use these equations to fit our data by using the substitution

$$v = 3.258\ diameter(nm) \qquad v \geq 2 \qquad \text{S.8}$$

Model used to fit the data

Full details of the model will be provided in a future publication, however the response is based around a previous paper of ours in which we provided a derivation of the Tafel Volmer equation in terms of the individual electrochemical rate constants. We use a Tafel-Volmer (TV) model instead of the Heyrovsky-Tafel-Volmer (HTV) model preferred by some others for modelling the HOR[3-6] as the HTV cannot replicate the formation of peaks (it can only show a plateau) and cannot produce the decrease in HOR performance at high overpotential, even if we include a reasonable anion adsorption contribution.

We solve the steady state equation for hydrogen coverage under the assumption that the maximum available surface is determined by the extent of site blocking. This means that the available free space for hydrogen adsorption is $(1-\theta_{\mathrm{Anion}}-\theta_{H_{\mathrm{ad}}})$ where $\theta_{H_{\mathrm{ad}}}$ is the coverage of adsorbed hydrogen and θ_{Anion} is associated with the species which blocks the site. We solve the steady state equation for hydrogen coverage at the equilibrium potential (see [7])

$$\frac{d\theta_{H_{\mathrm{ad}}}^{TV,eq}}{dt} = 2B^2(1-\theta_{anion}^{eq}-\theta_{H_{\mathrm{ad}}}^{TV,eq})^2 - Z\theta_{H_{\mathrm{ad}}}^{TV,eq} + BZ(1-\theta_{anion}^{eq}-\theta_{H_{\mathrm{ad}}}^{TV,eq}) - 2\left(\theta_{H_{\mathrm{ad}}}^{TV,eq}\right)^2 = 0 \quad \text{S.9}$$

where the parameters $B=\sqrt{\frac{a_{\mathrm{H2}}k_{+\mathrm{T}}}{k_{-\mathrm{T}}}}$ and $Z=\frac{k_{+V}^{\mathrm{eq}}}{k_{-\mathrm{T}}}$, and $k_{-V}^{eq}=\frac{\mathrm{B}k_{+V}^{eq}}{a_{H^+}}$. This provides us with an equation for the hydrogen coverage as a function of the parameters at the equilibrium potential (note that setting $\theta_{Anion}\to 0$ recovers the result we derived in [7]). In order to handle polarisation away from the equilibrium potential we substitute k_{+V}^{eq} and k_{-V}^{eq} with k_{+V} and k_{-V} such that

$$k_{+V}=k_{+V}^{\mathrm{eq}}e^{\beta f\eta} \quad \text{S.10}$$

$$k_{-V}=\frac{\mathrm{B}k_{+V}^{\mathrm{eq}}}{a_{H^+}}e^{-(1-\beta)\eta f} \quad \text{S.11}$$

where $f=\frac{F}{RT}$. Following this substitution the potential dependent equation for hydrogen coverage becomes

$$\theta_{H_{\mathrm{ad}}}^{TV}=\frac{1}{4(-1+B^2)}\left(Be^{(-1+\beta)\eta f}Z+e^{\beta\eta f}Z+4B^2(1-\theta_{\mathrm{anion}}) + \sqrt{-8B(-1+B^2)(1-\theta_{\mathrm{anion}})(e^{(-1+\beta)\eta f}Z+2B(1-\theta_{\mathrm{anion}}))+(Be^{(-1+\beta)\eta f}Z+e^{\beta\eta f}Z+4B^2(1-\theta_{\mathrm{anion}}))^2}\right) \quad \text{S.12}$$

θ_{Anion} takes the potential dependent form shown in Eq 6 (main paper). The current density is then determined by substitution of Eq S.12 into the kinetic equation for the electrochemical current density

$$j^{\mathrm{TV}}(\eta)=Fk_{\mathrm{des}}\left(Z\theta_{H_{\mathrm{ad}}}^{TV}e^{\beta\eta f}-BZ(1-\theta_{\mathrm{anion}}-\theta_{H_{\mathrm{ad}}}^{TV})e^{1(1-\beta)\eta f}\right) \quad \text{S.13}$$

As some of us have pointed out in a previous paper (see [7]), the link between the slope of the micropolarisation region and the exchange current density is more complex for multi-step reactions like the HOR/HER than provided for by the Butler Volmer equation, and we cannot simply use this slope to determine the exchange current density. Solution of the "true" exchange current density is obtained by determining the magnitude of the half currents at the equilibrium potential (i.e. taking one of the terms in Eq S.13 and setting $\eta=0$.

$$j_{0,true}=Fk_2^{\mathrm{eq}}\theta_{H_{ad}}^{TV,eq}\left(1-\theta_{anion}^{eq}\right) \quad \text{S.14}$$

When anion coverage is zero, this resolves to the result in our previous paper[7], and when $Z\to 0$, the slope of the linear polarisation region is. For the micropolarisation region, determining the first derivative of S.13 versus potential and setting the overpotential to zero allows us to determine the "effective" exchange current density from the micropolarisation region.

$$j_{0,micropol}^{TV}=\frac{RT}{F}\left(\frac{\partial j^{\mathrm{TV}}(\eta)}{\partial\eta}\right)_{\eta=0}=\frac{Fk_2^{\mathrm{eq}}\theta_{H_{ad}}^{TV,eq}\left(1-\theta_{anion}^{eq}\right)}{\frac{Z}{4\mathrm{B}\left(1-\theta_{anion}^{eq}\right)}+\frac{Z}{4\left(1-\theta_{anion}^{eq}\right)}+1} \quad \text{S.15}$$

When $\theta_{anion}^{eq}\to 0$, we obtain the same result as our previous paper[7], and when $Z\to 0$, the slope of the linear polarisation region is a good approximation to the true exchange current density (i.e. S.15 becomes S.14).

Fitting experimental data to model

All four data sets (i.e. four different particle sizes) were fit **simultaneously** in Excel utilising the Solver module and the GRG Nonlinear solver with constraints on the fitting values. The fit was optimised up to a potential of 0.5 V. Above this potential there was extra loss of the platinum surface area due to the presence of oxide, which was only fully reduced when the potential went below 0.5 V. The parameters fitted were B, Z, k_{des}, E'_{anion}, and λ_{anion} for each of the two sites (edge and facet). β, the molecular symmetry factor is fixed at ½. It is assumed that across all particles, these two sets of parameters remain the same, and that the only difference when particle size is changed was a difference in ratio of the two different sites. Hence, four extra fit parameters are used to specify the ratio of facet to edge for each of the different particles. Overall, there are fourteen parameters which were optimised in order to produce the four different curves in Figure 4. It was noticed that E'_{Anion} for facet sites could vary over a moderate range of potentials on either side of the best fit value, and only weakly affect the goodness of fit. This is probably associated with the relatively low charge transfer associated with anions on the facets.

Calculation of RDE response from simulated data

If we assume the curves we calculate and show in Figure 5A are mass transport free, we can calculate the expected response of an RDE electrode with an electrocatalyst with the same electrokinetic performance by using

$$\frac{1}{j(E)} = \frac{1}{j_{MT}(E)} + \frac{1}{j_{Facet}(E)} \quad \text{S.16}$$

where $j_{MT}(E)$ is the potential dependent mass transport limited current at E, and $j_{Facet}(E)$ is the mass transport free kinetic current for the facet. We cannot use the limiting value of j_{MT} as in the region we are interested in there is insufficient overpotential to drive the reaction to significant completion. $j_{MT}(E)$ is determined by assuming Fickian diffusion of the hydrogen to the electrode surface leading to a simple first order expression

$$j_{MT}(E) = 2\ F\ A\ k_{MT}(c_{H_2}^{Bulk} - c_{H_2}^{Surf}(E)) \quad \text{S.17}$$

Where A is the electrode area, $c_{H_2}^{Bulk}$ and $c_{H_2}^{Surf}$ are the concentrations of hydrogen in the bulk and at the surface respectively. $c_{H_2}^{Surf}$ is determined by inversion of the Nernst equation for the mass transport overpotential associated with depletion of hydrogen due to the reaction occurring at the electrode surface

$$E = E^{eq} - \eta_{MT} \quad \text{S.18}$$

$$\eta_{MT} = \frac{RT}{2F} log_e \frac{c_{H_2}^{Surf}}{c_{H_2}^{Bulk}} \quad \text{S.19}$$

k_{MT} is the mass transport rate constant and for an RDE is

$$k_{MT} = 0.62 D^{3/2} \nu^{-1/6} \omega^{1/2} \quad \text{S.20}$$

Where the parameters have their usual meaning and the rotation rate is in rad s^{-1}. Figure S2 shows the performance of an RDE electrode with an infinitely fast 2-electron reaction (i.e. the mass transport limited case), and that of the edges and facets respectively in the case of anion electrosorption occurring. It can be seen that the edge performance is indistinguishable from the "pure" RDE performance.

References

1. C. M. Zalitis, J. Sharman, E. Wright and A. R. Kucernak, *Electrochimica Acta*, 2015, **176**, 763-776.
2. K. Kinoshita, *Journal of The Electrochemical Society*, 1990, **137**, 845-848.
3. J. X. Wang, T. E. Springer and R. R. Adzic, *Journal of The Electrochemical Society*, 2006, **153**, A1732-A1740.
4. M. A. Montero, M. R. G. de Chialvo and A. C. Chialvo, *Electrochemistry Communications*, 2010, **12**, 398-401.
5. P. M. Quaino, M. R. G. de Chialvo and A. C. Chialvo, *Electrochimica Acta*, 2007, **52**, 7396-7403.
6. M. R. G. Dechialvo and A. C. Chialvo, *Journal of Electroanalytical Chemistry*, 1994, **372**, 209-223.
7. A. R. Kucernak and C. Zalitis, *The Journal of Physical Chemistry C*, 2016, **120**, 10721-10745.

